JGP Journal of General Physiology

COMMUNICATION

Excitation–Contraction Coupling

Acute exposure to extracellular BTP2 does not inhibit Ca^{2+} release during EC coupling in intact skeletal muscle fibers

Lan Wei-LaPierre[1], Linda Groom[2], and Robert T. Dirksen[2]

The inhibitor of store-operated Ca^{2+} entry (SOCE) BTP2 was reported to inhibit ryanodine receptor Ca^{2+} leak and electrically evoked Ca^{2+} release from the sarcoplasmic reticulum when introduced into mechanically skinned muscle fibers. However, it is unclear how effects of intracellular application of a highly lipophilic drug like BTP2 on Ca^{2+} release during excitation–contraction (EC) coupling compare with extracellular exposure in intact muscle fibers. Here, we address this question by quantifying the effect of short- and long-term exposure to 10 and 20 µM BTP2 on the magnitude and kinetics of electrically evoked Ca^{2+} release in intact mouse flexor digitorum brevis muscle fibers. Our results demonstrate that neither the magnitude nor the kinetics of electrically evoked Ca^{2+} release evoked during repetitive electrical stimulation were altered by brief exposure (2 min) to either BTP2 concentration. However, BTP2 did reduce the magnitude of electrically evoked Ca^{2+} release in intact fibers when applied extracellularly for a prolonged period of time (30 min at 10 µM or 10 min at 20 µM), consistent with slow diffusion of the lipophilic drug across the plasma membrane. Together, these results indicate that the time course and impact of BTP2 on Ca^{2+} release during EC coupling in skeletal muscle depends strongly on whether the drug is applied intracellularly or extracellularly. Further, these results demonstrate that electrically evoked Ca^{2+} release in intact muscle fibers is unaltered by extracellular application of 10 µM BTP2 for <25 min, validating this use to assess the role of SOCE in the absence of an effect on EC coupling.

Introduction

N-[4-[3,5-bis(trifluoromethyl)-1H-pyrazol-1-yl]phenyl]-4-methyl-1,2,3-thiadiazole-5-carboxamide (BTP2 or YM58483) is a Ca^{2+} release–activated Ca^{2+} (CRAC) channel inhibitor (Zitt et al., 2004) commonly used to assess the role of store-operated Ca^{2+} entry (SOCE). BTP2 inhibits SOCE activity through effects on both Orai1 and canonical transient receptor potential 3 (TRPC3) channels (He et al., 2005). Previous studies of SOCE in skeletal muscle cells have used 5–10 µM extracellular BTP2 to inhibit SOCE in intact myotubes (Eltit et al., 2013; Eltit et al., 2011; Li et al., 2010; Yarotskyy and Dirksen, 2012), acutely dissociated adult muscle fibers (Michelucci et al., 2019; Michelucci et al., 2020; Wei-LaPierre et al., 2013), and whole muscles (Boncompagni et al., 2017; Boncompagni et al., 2021). In the first issue of the *Journal of General Physiology* in 2021, Meizoso-Huesca and Launikonis (2021) published an intriguing study that re-examines the effect of BTP2 on Ca^{2+} handling in mechanically skinned rat extensor digitorum longus (EDL) muscle fibers. This study found that apart from its known ability to inhibit SOCE, BTP2 also inhibited both basal ryanodine receptor Ca^{2+} leak and evoked Ca^{2+} release (caused by either exposure to low intracellular Mg^{2+} or electrical stimulation). Specifically, the authors reported that both type 1 ryanodine receptor (RYR1) Ca^{2+} leak and Ca^{2+} release induced by exposure to low intracellular Mg^{2+}, presumably due to activation of RYR1 in the SR, were reduced when 10 µM BTP2 was applied either intracellularly or in the extracellular solution (trapped within sealed transverse tubules [T-tubules] of the skinned fiber). While potential irreversible effects of intracellular BTP2 contamination that occur during

[1]Department of Applied Physiology and Kinesiology, University of Florida, Gainesville, FL; [2]Department of Pharmacology and Physiology, University of Rochester Medical Center, Rochester, NY.

Correspondence to Robert T. Dirksen: Robert_Dirksen@URMC.rochester.edu

This work is part of a special issue on excitation–contraction coupling.

mechanical skinning in the presence of BTP2 were not addressed, the authors concluded that BTP2 inhibits RYR1 channel activity regardless of the route of application. Importantly, Meizoso-Huesca and Launikonis (2021) also found that Ca^{2+} transients in skinned fibers elicited during repetitive (0.5 Hz) electrical twitch stimulation were essentially abolished following intracellular application of either 10 µM BTP2 (within ∼60 s) and 20 µM BTP2 (<10 s). The authors also provided evidence suggesting that this inhibition was unlikely the result of direct inhibition of RYR1 channels, but was dependent on the integrity of T-tubule and/or critical protein–protein interactions within the triad junction.

The results of Meizoso-Huesca and Launikonis (2021) have potentially important implications for interpreting results from prior studies that have used BTP2 as one means of assessing the relative role of SOCE in sustained Ca^{2+} transient amplitude (Michelucci et al., 2019; Wei-LaPierre et al., 2013) and contractile force production (Boncompagni et al., 2017; Boncompagni et al., 2021) during repetitive electrical stimulation. However, a significant limitation of this study is that the authors only tested the effect of intracellular applied BTP2 on electrically evoked Ca^{2+} release in mechanically skinned muscle fibers. Parallel studies on the effect of extracellular BTP2 on electrically evoked Ca^{2+} release in intact (or skinned) fibers were not completed. Such studies are critical since extracellular BTP2 is typically used to assess the relative role of SOCE on muscle physiology in intact myotubes, single fibers, and whole muscles, or even following systemic treatment of live animals (Zhao et al., 2012). Therefore, we determined the effect of extracellular BTP2 on electrically evoked RYR1 Ca^{2+} release during excitation–contraction (EC) coupling in single intact mouse muscle fibers following short-term exposure (2 min) using the same BTP2 concentrations and stimulation protocol employed by Meizoso-Huesca and Launikonis (2021). In addition, since BTP2 is highly lipophilic, the drug may cross the plasma membrane slowly over time to reach intracellular compartments when applied extracellularly. Therefore, we also examined the effect of prolonged exposure of extracellular BTP2 (30 min) in intact muscle fibers. The results provide important concentration and exposure guidance with regard to the proper use of BTP2 to inhibit preferentially SOCE in intact skeletal muscle fibers.

Materials and methods

Animals

All experiments used 4-mo-old male and female C57BL6/J wild-type mice. Mice were group-housed in sterile ventilated micro-isolator cages on corncob bedding in the University of Rochester Medical Center vivarium, an Association for Assessment and Accreditation of Laboratory Animal Care International–accredited facility. All animal procedures were approved by the University Committee on Animal Resources at the University of Rochester.

Reagents

All chemicals and dyes were purchased from Sigma-Aldrich or Invitrogen. Stock concentrations of mag-fluo-4-AM (1 mM) and BTP2 (10 mM) were made up in DMSO and then diluted to their respective final concentrations in Ringer's solution consisting of (in mM) 146 NaCl, 5 KCl, 2 $CaCl_2$, 1 $MgCl_2$, and 10 HEPES, pH 7.4). The efficiency of BTP2 to block SOCE at the concentrations used in this study was validated in Mn^{2+} quench studies as described previously (Michelucci et al., 2019; Wei-LaPierre et al., 2013).

Measurements of electrically evoked intracellular Ca^{2+} transients in intact flexor digitorum brevis (FDB) fibers

Acutely dissociated FDB fibers were isolated from mouse footpads before experiments using enzymatic digestion as previously described (Lueck et al., 2007). Single intact FDB fibers were plated on glass-bottom dishes and loaded with low-affinity Ca^{2+} dye, mag-fluo-4 (4 µM), in Ringer's solution for 20 min at room temperature. Following 20 min incubation in dye-free Ringer's supplemented with 25 µM N-benzyl-p-toluene sulfonamide, a skeletal muscle myosin inhibitor to reduce movement artifacts during stimulation, fibers were mounted on the stage of a Nikon Eclipse 2000E inverted microscope. Twitch electrical stimulation was delivered to individual FDB fibers using a NaCl-filled glass electrode placed adjacent to the cell of interest. For short-term BTP2 exposure, FDB fibers were stimulated at a frequency of 0.5 Hz for a total of 3 min, where control Ringer's was perfused during the initial 60 s followed by 2 min in Ringer's solution supplemented with DMSO vehicle, 10 µM BTP2, or 20 µM BTP2. For BTP2 application, a local perfusion system that enabled fast and complete solution exchange within 5 s was employed with a perfusion barrel placed adjacent to the fiber of interest. Throughout the stimulation period, mag-fluo-4 fluorescence within a selected portion of the fiber interior was excited at 480 ± 15 nm using an Excite epifluorescence illumination system (Nikon Instruments). Fluorescence emission at 535 ± 30 nm was monitored using a 40× oil objective and photomultiplier detection system (Photon Technologies Inc.). For prolonged BTP2 exposure, FDB fibers were continuously stimulated at a frequency of 0.1 Hz for 30 min in the presence of DMSO vehicle, 10 µM BTP2, or 20 µM BTP2. During the stimulation period, mag-fluo-4 fluorescence was acquired for four successive transients every 5 min, while keeping the computer-controlled shutter closed in between data collection in order to minimize fiber phototoxicity and photobleaching of the dye. Relative changes in mag-fluo-4 fluorescence from baseline ($\Delta F/F_0$) were digitized at 10 kHz and analyzed using Clampfit 10.0 (Molecular Devices) and Igor (Wave Metrics) software.

Data and statistical analyses

The peak change in $\Delta F/F_0$ during electrical stimulation was determined for each twitch Ca^{2+} transient throughout the 3-min period of short-term BTP2 exposure and averaged across the four successive twitch Ca^{2+} transients acquired at 5-min intervals during long-term BTP exposure. Kinetic analyses of the rise and decay phases of the transients elicited during short-term exposure were assessed from the average of the last five transients in control Ringer's solution (before addition of DMSO or BTP2) and the final five transients after 2 min exposure to either DMSO or BTP2.

The maximum rate of electrically evoked Ca^{2+} release was approximated from the peak of the first derivative of the

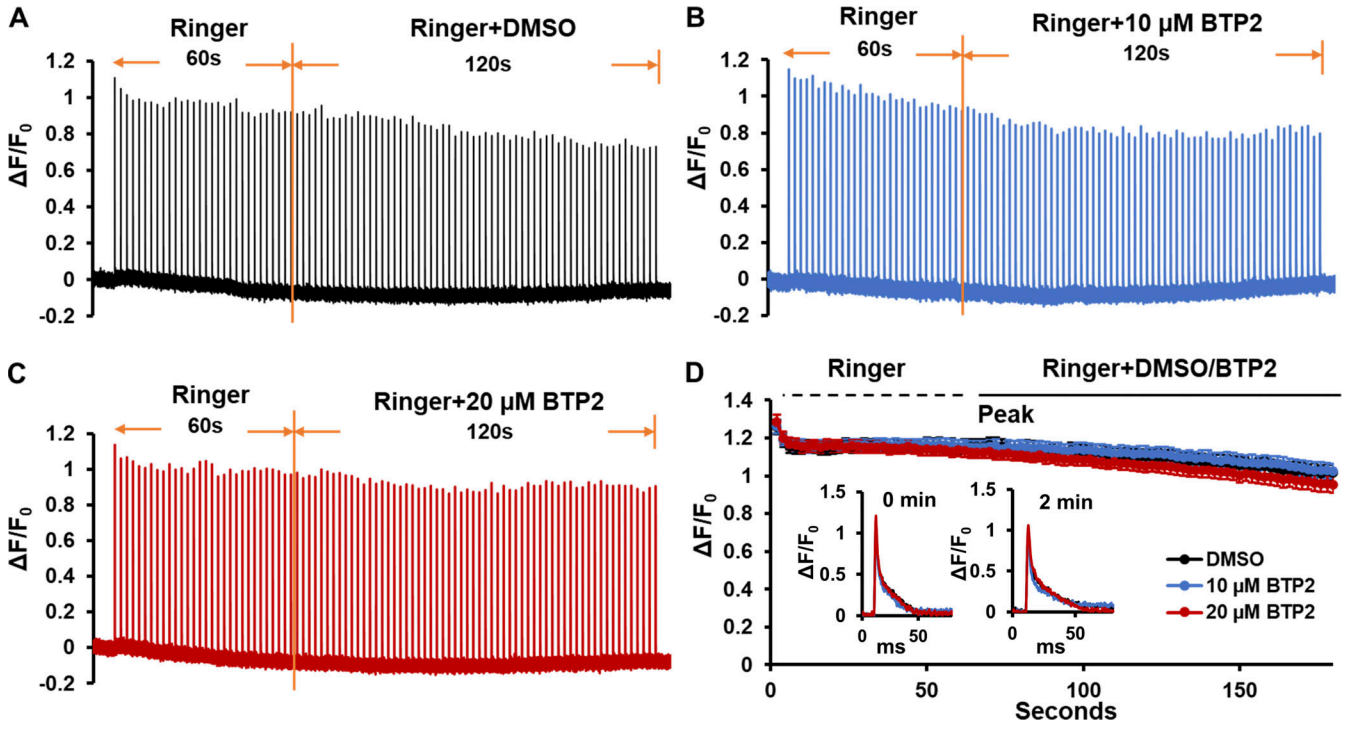

Figure 1. **Electrically evoked Ca^{2+} transients in intact FDB fibers during acute exposure to BTP2. (A–C)** Representative mag-fluo-4 traces during 180 s of continuous electrically evoked twitch stimulation (0.5 Hz), starting with a 60-s perfusion with control Ringer's solution followed by 120 s application of DMSO control (A), 10 µM BTP2 (B), or 20 µM BTP2 (C) in Ringer's solution. **(D)** Average (± SEM) peak $\Delta F/F_0$ throughout the 180 s of continuous stimulation. Inset: Representative traces of electrically evoked mag-fluo-4 transients before (0 min) and at the end (2 min) of DMSO or BTP2 exposure. *n* = 18–36 cells from three to five mice; one-way ANOVA with Tukey post hoc test.

mag-fluo-4 fluorescence (dF/dt) during electrical stimulation. The decay phase of each transient was fitted according to the following second order exponential equation and used to generate average values both before and after DMSO or BTP2 exposure:

$$F(t) = A_{fast} \times \left[\exp\left(-t/\tau_{fast}\right)\right] + A_{slow} \times \left[\exp\left(-t/\tau_{slow}\right)\right],$$

where F(t) is the fluorescence at time t, A_{fast} and τ_{fast} are the amplitude and time constants of the fast component, respectively, and A_{slow} and τ_{slow} are the amplitude and time constants of the slow component, respectively.

All data groups were verified to follow a normal distribution before conducting parametric statistical analyses using the Prism (GraphPad) software. One-way ANOVA with post hoc Tukey test was used to statistically compare peak amplitude data. Two-way ANOVA with post hoc Tukey test was used for statistical analysis of the kinetic components of Ca^{2+} transient. All data were expressed as mean ± SEM with $P < 0.05$ considered statistically significant.

Results

Short-term exposure to extracellular BTP2 does not alter the amplitude of electrically evoked Ca^{2+} release in intact FDB fibers

Prior studies used 10 µM BTP2 to inhibit SOCE in intact fibers (Michelucci et al., 2019; Michelucci et al., 2020; Wei-LaPierre et al., 2013) and whole muscles (Boncompagni et al., 2017; Boncompagni et al., 2021). Using the stimulation paradigm of Meizoso-Huesca and Launikonis (2021), extracellular application of 10 µM BTP2 did not significantly alter the magnitude of electrically evoked Ca^{2+} release compared with control even after 2 min (peak $\Delta F/F_0$: 1.02 ± 0.04 for DMSO and 1.02 ± 0.04 for 10 µM BTP2; Fig. 1, A, B, and D). In fact, electrically evoked Ca^{2+} transient amplitude was also not significantly altered 2 min after exposure to even 20 µM BTP2 (peak $\Delta F/F_0$: 0.93 ± 0.06 for 20 µM BTP2; Fig. 1, C and D). As a result, peak Ca^{2+} transient amplitudes were not significantly different for any time point across all groups throughout the entire 3-min stimulation period (Fig. 1 D).

Short-term exposure to extracellular BTP2 does not alter the kinetics of electrically evoked Ca^{2+} release in intact FDB fibers

Superimposed traces from FDB fibers before (Fig. 2 A) and 2 min after (Fig. 2 B) treatment with vehicle (DMSO), 10 µM, and 20 µM BTP2 exhibited a similar rate of rise. Similarly, the rate of rise of the transient was also comparable in FDB fibers before and after exposure for 2 min to DMSO (Fig. 2 C), 10 µM (Fig. 2 D), or 20 µM BTP2 (Fig. 2 E). To better quantify this, the maximum rate of electrically evoked Ca^{2+} release was approximated from the peak dF/dt of the mag-fluo-4 fluorescence. This analysis revealed that peak dF/dt was not significantly different between FDB fibers 2 min after exposure to vehicle control (DMSO), 10 µM, or 20 µM BTP2 (Fig. 3 D).

In addition, the transient decay kinetics were also similar for all conditions in control (Fig. 2 F) and 2 min after exposure

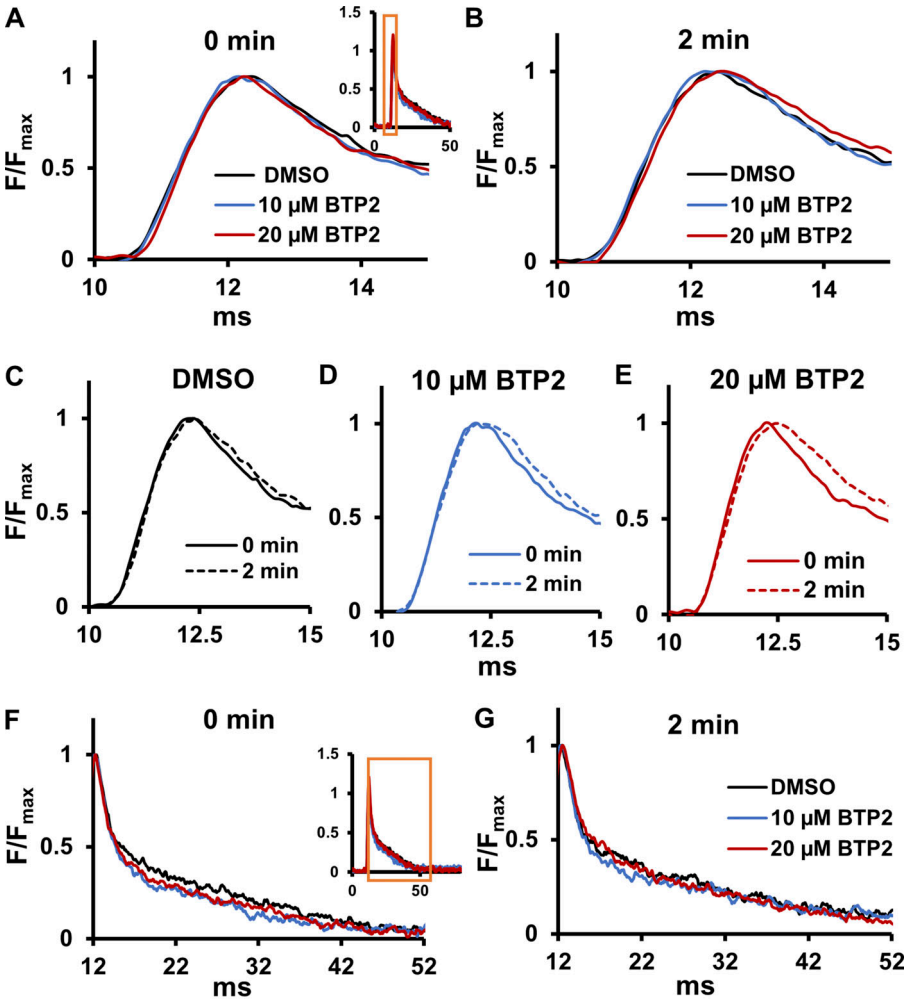

Figure 2. **Superimposed traces of electrically evoked Ca^{2+} transients in intact FDB fibers on an expanded time scale. (A and B)** Overlay of representative mag-fluo-4 traces with the rising phase on an expanded time scale for the fibers presented in the inset to Fig. 1 D before (0 min; A) and after (2 min; B) exposure to DMSO (black), 10 μM BTP2 (blue), or 20 μM BTP2 (red). Inset in A indicates the region of the traces (in orange box) presented on the expanded time scale in A–E. **(C–E)** Overlay of representative superimposed traces on an expanded time scale before and after 2 min exposure to DMSO (C), 10 μM BTP2 (D), or 20 μM BTP2 (E). **(F and G)** Overlay of the decay phase of mag-fluo-4 traces on an expanded time scale for the representative fibers presented in the inset to Fig. 1 D before (0 min; F) and after (2 min; G) exposure to DMSO (black), 10 μM BTP2 (blue), and 20 μM BTP2 (red). Inset in panel F indicates the region of the traces (in orange box) presented on the expanded time scale in F and G. Fluorescence (F) of the representative traces was normalized to the peak fluorescence (F_{max}) for each fiber.

(Fig. 2 G). The decay phase of the electrically evoked mag-fluo-4 transients is well-described by a double exponential fit where the fast component of decay primarily reflects Ca^{2+} binding to fast myoplasmic Ca^{2+} buffers and the slow component of decay is dominated by SERCA pump-mediated reuptake (Baylor and Hollingworth 2003; Capote et al., 2005; Carroll et al., 1999). Thus, we fit the decay phase of the transients with a double exponential equation to quantify the fast (A_{fast} and τ_{fast}) and slow (A_{slow} and τ_{slow}) components before and after treatment with vehicle, 10 μM, and 20 μM BTP2 (representative traces and corresponding double exponential fits shown in Fig. 3, A–C). No statistically significant differences in the fast or slow amplitudes of decay (Fig. 3 E), the fast time constant of decay (Fig. 3 F), or the slow time constant of decay (Fig. 3 G) were observed between fibers exposed to DMSO (vehicle), 10 μM BTP2, or 20 μM BTP2. While some time-dependent differences (e.g., between 0 and 2 min) were observed in the fast amplitude of decay, these were not pursued further as the changes were similar across all treatment groups. The above results indicate that the magnitude and kinetics of electrically evoked Ca^{2+} release during EC coupling in intact FDB fibers is not significantly altered following short-term (2 min) exposure to either 10 μM BTP2 or 20 μM BTP2.

Prolonged exposure to extracellular BTP2 reduces the amplitude of electrically evoked Ca^{2+} release in a concentration- and time-dependent manner

Given the highly lipophilic properties of BTP2, prolonged extracellular exposure would be expected to result in an initial partition into surface and T-tubule membranes followed by slower diffusion across the sarcolemma to nearby intracellular compartments. To investigate this possibility, we examined the effect of prolonged exposure to DMSO, 10 μM BTP2, or 20 μM BTP2 (up to 30 min) on electrically evoked Ca^{2+} transients in intact FDB fibers. For these studies, FDB fibers were stimulated at a lower frequency (0.1 Hz), and mag-fluo-4 fluorescence was monitored for several successive transients every 5 min with the shutter closed in between recording intervals (to minimize phototoxicity/bleaching). Extracellular application of 10 μM BTP2 did not significantly alter peak Ca^{2+} transient amplitude from that of vehicle control (DMSO) until after 25 min of exposure (Fig. 4, blue traces and blue bars). In contrast, peak Ca^{2+} transient amplitude was significantly reduced as early as 5 min after exposure to 20 μM BTP2, which then continued to decline in a time-dependent manner, reaching ~20% of DMSO control after 30 min (Fig. 4, red traces and red bars).

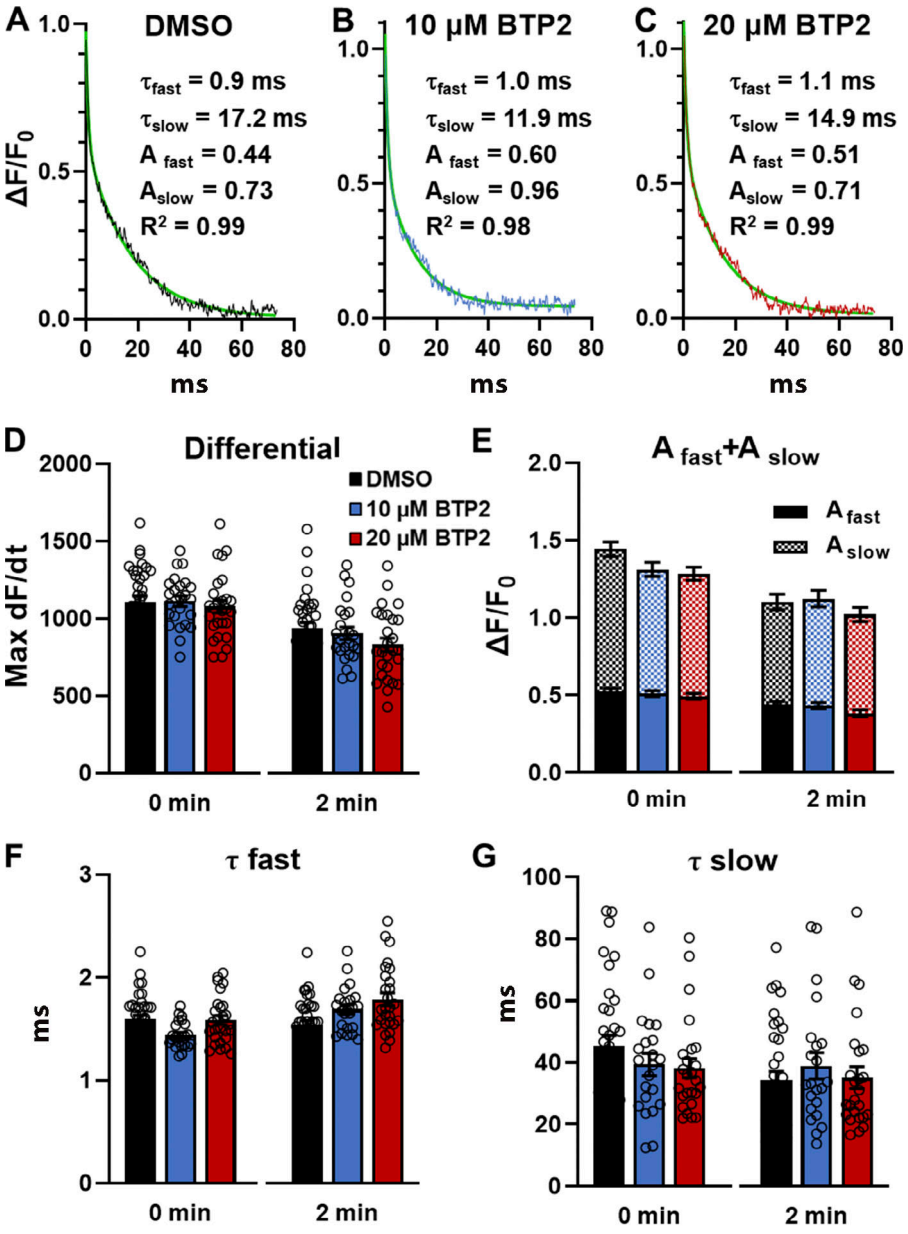

Figure 3. **Kinetic analyses of electrically evoked Ca^{2+} transients in intact FDB fibers after acute exposure to BTP2. (A–C)** Representative mag-fluo-4 traces with the decay phase shown on an expanded time scale and fitted with a double exponential equation (green lines) from FDB fibers before exposure to DMSO (A), 10 µM BTP2 (B), or 20 µM BTP2 (C). Insets: Fitted parameters for each condition, including the fast and slow amplitudes of decay (A_{fast} and A_{slow}), fast and slow time constants of decay (τ_{fast} and τ_{slow}), and goodness of fit values (R^2). **(D)** Average (± SEM) maximal mag-fluo-4 transient rate of rise (Max dF/dt) before (0 min) and after (2 min) exposure to DMSO control (black), 10 µM BTP2 (blue), or 20 µM BTP2 (red). **(E)** Averaged (± SEM) peak amplitudes of the fast (A_{fast}, solid bars) and slow (A_{slow}, checked bars) components of the decay phase of the mag-fluo-4 transient before and 2 min after exposure to DMSO control (black), 10 µM BTP2 (blue), or 20 µM BTP2 (red). **(F and G)** Average (± SEM) fast (τ_{fast}; F) and slow (τ_{slow}; G) time constants of the decay phase of the mag-fluo-4 transient before and 2 min after exposure to DMSO control (black), 10 µM BTP2 (blue), or 20 µM BTP2 (red). *n* = 12–36 cells from three to five mice for each group; two-way ANOVA with Tukey post hoc test. P = 0.37–0.99 for pairwise post hoc comparisons in D; P = 0.41–0.99 for pairwise comparisons in E; P = 0.08–0.99 for pairwise comparisons in F; P = 0.67–0.99 for post hoc comparisons in G.

Discussion

The primary finding of this communication is that electrically evoked Ca^{2+} release in intact mouse FDB fibers is unaltered by extracellular application of 10 µM BTP2 for up to 25 min (Figs. 1, 2, and 3). These findings indicate that EC coupling is unaltered by BTP2 exposure conditions used previously to inhibit SOCE in intact muscle preparations (Boncompagni et al., 2017; Boncompagni et al., 2021; Eltit et al., 2013; Li et al., 2010; Yarotskyy and Dirksen, 2012; Zhao et al., 2012; Eltit et al., 2011; Wei-LaPierre et al., 2013; Michelucci et al., 2019; Michelucci et al., 2020). Moreover, these results are also consistent with prior findings that SOCE does not significantly contribute to Ca^{2+} transients during EC coupling (Koenig et al., 2018; Meizoso-Huesca and Launikonis, 2021).

Consistent with these results, we previously reported that inhibition of SOCE by exposure to 10 µM BTP2 for 2.5–10 min does not alter peak electrically evoked Ca^{2+} release in intact FDB fibers (Wei-LaPierre et al., 2013) or peak specific force production in intact muscle (Michelucci et al., 2019) during a single high-frequency stimulation train. Similar results were observed following inducible, muscle-specific Orai1 knockout (Carrell et al., 2016; Michelucci et al., 2019). However, inhibition of SOCE increases fatigability during repetitive high-frequency stimulation, which is reflected in both a reduction in Ca^{2+} transient amplitude following short-term exposure (<10 min) to 10 µM BTP2 (Wei-LaPierre et al., 2013) and muscle-specific force production following inducible ablation of Orai1 (Michelucci et al., 2019). These studies used the same stimulation paradigm (500-ms stimulations delivered at 50 Hz, repeated every 2.5 s) and verified that inhibition of SOCE (both pharmacologically and genetically) results in a comparable increase in fatigue during repetitive high-frequency stimulation. The finding in

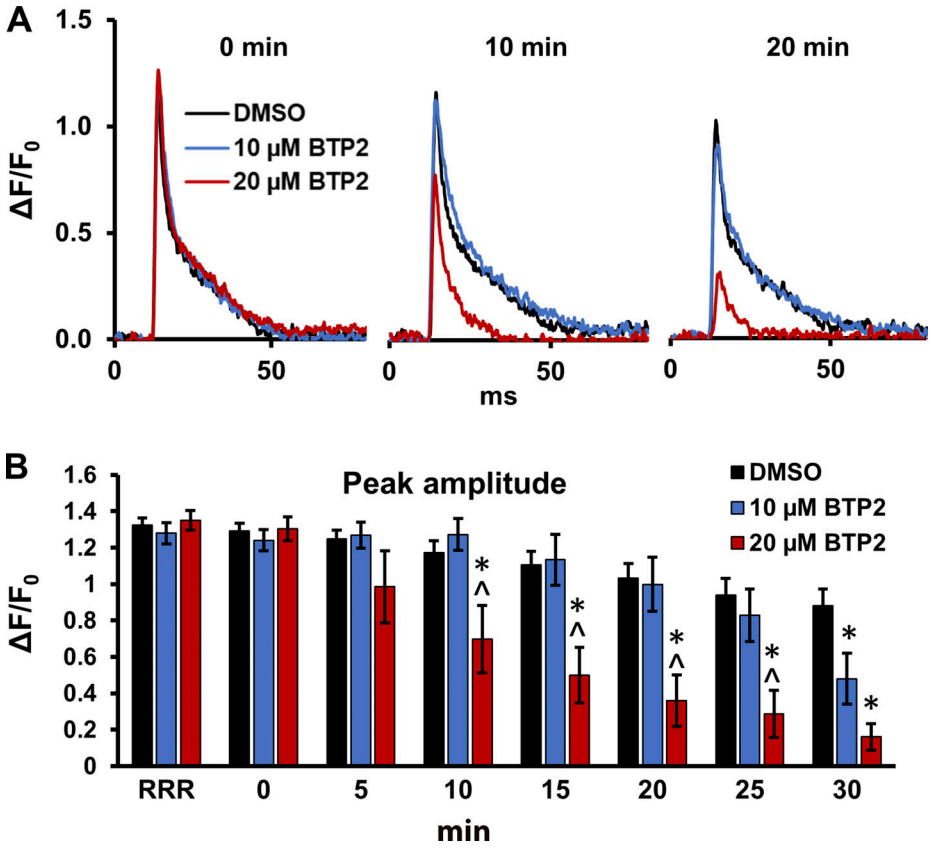

Figure 4. **Electrically evoked Ca^{2+} transients in intact FDB fibers during prolonged exposure to BTP2. (A)** Representative mag-fluo-4 traces before (0 min, left), after 10 min exposure (middle), and after 20 min exposure (right) to DMSO (black), 10 μM BTP2 (blue), or 20 μM BTP2 (red) during continuous electrical stimulation for 30 min at 0.1 Hz. **(B)** Average (± SEM) peak $\Delta F/F_0$ at 5-min intervals throughout 30 min exposure to DMSO (black bars), 10 μM BTP2, (blue bars), or 20 μM BTP2 (red bars). *n* = 13–26 cells from three mice. *, Significantly different from DMSO; P = 0.0069 for 10 min; P = 0.0012 for 15 min; P = 0.0004 for 20 min; P = 0.0009 for 25 min; P < 0.0001 for 30 min, 20 μM BTP2; and P = 0.0215 for 30 min, 10 μM BTP2. ^, Significantly different from 10 μM BTP2; P = 0.0031 for 10 min; P = 0.0025 for 15 min; P = 0.0026 for 20 min; and P = 0.0151 for 25 min.

this communication supports these previous studies by demonstrating that short-term exposure (<30 min) of intact FDB fibers to 10 μM BTP2 does not significantly affect Ca^{2+} release during EC coupling. Thus, effects of acute exposure in intact fibers/muscle up to 10 μM BTP2 reported previously are not due to effects of the drug on RYR1-mediated Ca^{2+} release during EC coupling.

While Ca^{2+} release during EC coupling is not reduced following short-term exposure to 10 μM BTP2, it is reduced for longer exposures to 10 μM BTP2 (>30 min) and for shorter exposures to 20 μM BTP2 (>5 min). While peak Ca^{2+} transient amplitude is reduced in the presence of 20 μM BTP2 after ∼30 action potentials at 0.1 Hz (5 min, Fig. 4), it is unaltered at this concentration after 60 action potentials applied at a higher frequency over a shorter period of time (0.5 Hz in 2 min, Fig. 1). These results indicate that the inhibitory effect of BTP2 on Ca^{2+} release during EC coupling is primarily concentration- and time-dependent rather than use-dependent, consistent with delayed access to intracellular compartments when applied to intact fibers. Together, our studies provide critical evidence to support the use of 10 μM BTP2 for up to 25 min for physiological studies of SOCE activity in intact muscle fibers.

Our findings of the absence of any effect of 2 min exposure to 10–20 μM on EC coupling in intact muscle fibers (Fig. 1) are in marked contrast to those reported by Meizoso-Huesca and Launikonis (2021) in mechanically skinned rat EDL muscle fibers. In skinned fibers, intracellular application of 10 μM BTP2 reduced electrically evoked Ca^{2+} release (0.5 Hz stimulation) ∼50% after 20–25 s, and 20 μM BTP2 essentially abolished Ca^{2+} release in <10 s. The results of our prolonged BTP2 exposure experiments in intact fibers (Fig. 4) suggest that the discrepancy between our results and those of Meizoso-Huesca and Launikonis (2021) is most likely due to the method of BTP2 application (extracellular versus intracellular). However, potential differences in species (mouse versus rat), muscle (FDB versus EDL), and experimental paradigms (intact versus skinned fibers) used cannot be excluded. Whatever the reason, our results demonstrate that caution needs to be taken when extrapolating effects of agents applied to the intracellular solution in skinned fiber preparations compared with extracellular application of the same agent in intact fibers.

Meizoso-Huesca and Launikonis (2021) proposed that BTP2 inhibition of RYR1 was independent of whether the compound was applied intracellularly or extracellularly as Ca^{2+} release induced during exposure to low intracellular Mg^{2+} was similarly reduced regardless of the orientation of BTP2 application. However, the inhibition of electrically evoked Ca^{2+} release by intracellular application of BTP2 reported by Meizoso-Huesca

and Launikonis (2021) was not repeated under conditions when BTP2 application was restricted to the extracellular space. As BTP2 is highly lipophilic, the compound preferentially partitions into membranes. When applied extracellularly, the drug will primarily partition into sarcolemmal and T-tubule membranes. Our results observed following prolonged exposure of intact fibers to BTP2 support the possibility that the compound may only slowly cross sarcolemmal and T-tubule membranes and diffuse into intracellular membranes during prolonged exposure. It is unclear in the study by Meizoso-Huesca and Launikonis (2021) precisely how long BTP2 was trapped in the T-tubule before the Ca^{2+} measurements were made. In addition, potential local intracellular accumulation of BTP2 cannot be excluded in these studies since the previously applied drug was present during mechanical skinning.

In summary, our results validate the use of 10 µM BTP2 for up to 25 min as a means of preferentially inhibiting SOCE in intact mouse FDB fibers in the absence of a significant impact on Ca^{2+} release during EC coupling.

Acknowledgments

Eduardo Ríos served as editor.

This work was supported by a grant from the National Institutes of Health (AR059646 to R.T. Dirksen).

The authors declare no competing financial interests.

Author contributions: L. Wei-LaPierre, conceptualization, data curation, formal analysis, visualization, and writing–original draft, review, and editing; L. Groom, data curation, formal analysis, investigation, project administration, visualization, and writing–review and editing; and R.T. Dirksen, conceptualization, funding acquisition, supervision, visualization, and writing–original draft, review, editing.

Submitted: 3 June 2021
Accepted: 30 November 2021

References

Baylor, S.M., and S. Hollingworth. 2003. Sarcoplasmic reticulum calcium release compared in slow-twitch and fast-twitch fibres of mouse muscle. *J. Physiol.* 551:125–138. https://doi.org/10.1113/jphysiol.2003.041608

Boncompagni, S., A. Michelucci, L. Pietrangelo, R.T. Dirksen, and F. Protasi. 2017. Exercise-dependent formation of new junctions that promote STIM1-Orai1 assembly in skeletal muscle. *Sci. Rep.* 7:14286. https://doi.org/10.1038/s41598-017-14134-0

Boncompagni, S., C. Pecorai, A. Michelucci, L. Pietrangelo, and F. Protasi. 2021. Long-Term Exercise Reduces Formation of Tubular Aggregates and Promotes Maintenance of Ca^{2+} Entry Units in Aged Muscle. *Front. Physiol.* 11:601057. https://doi.org/10.3389/fphys.2020.601057

Capote, J., P. Bolaños, R.P. Schuhmeier, W. Melzer, and C. Caputo. 2005. Calcium transients in developing mouse skeletal muscle fibres. *J. Physiol.* 564:451–464. https://doi.org/10.1113/jphysiol.2004.081034

Carrell, E.M., A.R. Coppola, H.J. McBride, and R.T. Dirksen. 2016. Orai1 enhances muscle endurance by promoting fatigue-resistant type I fiber content but not through acute store-operated Ca^{2+} entry. *FASEB J.* 30:4109–4119. https://doi.org/10.1096/fj.201600621R

Carroll, S., P. Nicotera, and D. Pette. 1999. Calcium transients in single fibers of low-frequency stimulated fast-twitch muscle of rat. *Am. J. Physiol.* 277:C1122–C1129. https://doi.org/10.1152/ajpcell.1999.277.6.C1122

Eltit, J.M., H. Li, C.W. Ward, T. Molinski, I.N. Pessah, P.D. Allen, and J.R. Lopez. 2011. Orthograde dihydropyridine receptor signal regulates ryanodine receptor passive leak. *Proc. Natl. Acad. Sci. USA.* 108:7046–7051. https://doi.org/10.1073/pnas.1018380108

Eltit, J.M., X. Ding, I.N. Pessah, P.D. Allen, and J.R. Lopez. 2013. Nonspecific sarcolemmal cation channels are critical for the pathogenesis of malignant hyperthermia. *FASEB J.* 27:991–1000. https://doi.org/10.1096/fj.12-218354

He, L.-P., T. Hewavitharana, J. Soboloff, M.A. Spassova, and D.L. Gill. 2005. A functional link between store-operated and TRPC channels revealed by the 3,5-bis(trifluoromethyl)pyrazole derivative, BTP2. *J. Biol. Chem.* 280:10997–11006. https://doi.org/10.1074/jbc.M411797200

Koenig, X., R.H. Choi, and B.S. Launikonis. 2018. Store-operated Ca^{2+} entry is activated by every action potential in skeletal muscle. *Commun. Biol.* 1:31. https://doi.org/10.1038/s42003-018-0033-7

Li, H., X. Ding, J.R. Lopez, H. Takeshima, J. Ma, P.D. Allen, and J.M. Eltit. 2010. Impaired Orai1-mediated resting Ca^{2+} entry reduces the cytosolic $[Ca^{2+}]$ and sarcoplasmic reticulum Ca^{2+} loading in quiescent junctophilin 1 knock-out myotubes. *J. Biol. Chem.* 285:39171–39179. https://doi.org/10.1074/jbc.M110.149690

Lueck, J.D., A. Mankodi, M.S. Swanson, C.A. Thornton, and R.T. Dirksen. 2007. Muscle chloride channel dysfunction in two mouse models of myotonic dystrophy. *J. Gen. Physiol.* 129:79–94. https://doi.org/10.1085/jgp.200609635

Meizoso-Huesca, A., and B.S. Launikonis. 2021. The Orai1 inhibitor BTP2 has multiple effects on Ca^{2+} handling in skeletal muscle. *J. Gen. Physiol.* 153:e202012747. https://doi.org/10.1085/jgp.202012747

Michelucci, A., S. Boncompagni, L. Pietrangelo, M. García-Castañeda, T. Takano, S. Malik, R.T. Dirksen, and F. Protasi. 2019. Transverse tubule remodeling enhances Orai1-dependent Ca^{2+} entry in skeletal muscle. *eLife.* 8:e47576. https://doi.org/10.7554/eLife.47576

Michelucci, A., S. Boncompagni, L. Pietrangelo, T. Takano, F. Protasi, and R.T. Dirksen. 2020. Pre-assembled Ca^{2+} entry units and constitutively active Ca^{2+} entry in skeletal muscle of calsequestrin-1 knockout mice. *J. Gen. Physiol.* 152. e202012617. https://doi.org/10.1085/jgp.202012617

Wei-LaPierre, L., E.M. Carrell, S. Boncompagni, F. Protasi, and R.T. Dirksen. 2013. Orai1-dependent calcium entry promotes skeletal muscle growth and limits fatigue. *Nat. Commun.* 4:2805. https://doi.org/10.1038/ncomms3805

Yarotskyy, V., and R.T. Dirksen. 2012. Temperature and RyR1 regulate the activation rate of store-operated Ca^{2+} entry current in myotubes. *Biophys. J.* 103:202–211. https://doi.org/10.1016/j.bpj.2012.06.001

Zhao, X., J.G. Moloughney, S. Zhang, S. Komazaki, and N. Weisleder. 2012. Orai1 mediates exacerbated $Ca^{(2+)}$ entry in dystrophic skeletal muscle. *PLoS One.* 7:e49862. https://doi.org/10.1371/journal.pone.0049862

Zitt, C., B. Strauss, E.C. Schwarz, N. Spaeth, G. Rast, A. Hatzelmann, and M. Hoth. 2004. Potent inhibition of Ca^{2+} release-activated Ca^{2+} channels and T-lymphocyte activation by the pyrazole derivative BTP2. *J. Biol. Chem.* 279:12427–12437. https://doi.org/10.1074/jbc.M309297200